Electronic Supplementary Material (ESI) for Journal of Materials Chemistry A.

A self-assembled intercalated metal–organic framework electrode with outstanding area capacity for high volumetric energy asymmetric capacitors

Nobuhiro Ogihara*, Yuka Ozawa and Osamu Hiruta

correspondence to: ogihara@mosk.tytlabs.co.jp

Supplementary Information

Supplementary Text

Supplementary Figures S1 to S10

Supplementary Text

Impedance theory

For a non-faradaic process at porous electrodes, the overall impedance is expressed as in eqn (S1).[1-4]

$$Z_{\omega} = \sqrt{\frac{R_{\mathrm{ion},\,L}}{j\omega C_{\mathrm{dl},\,A} \cdot 2\pi r}} \coth \sqrt{R_{\mathrm{ion},\,L} \cdot j\omega C_{\mathrm{dl},\,A} \cdot 2\pi r} L \qquad \text{(S1)}$$

The limiting values of the real (Z'_{ω}) as $\omega \rightarrow 0$ are shown by eqn (S2),

$$Z'_{\omega \to 0} = \frac{R_{\mathrm{ion}}}{3} \qquad \text{(S2)}$$

where R_{ion} is the mobility of Li ions inside the porous electrodes. Also R_{ion} can be expressed as shown by eqns. (S3) and (S4).

$$R_{ion} = R_{ion,L} \times \frac{L}{n} \qquad \text{(S3)}$$

$$R_{ion,L} = \frac{\rho}{\pi r^2} \qquad \text{(S4)}$$

From the mathematical equation, R_{ion} increases linearly with electrode thickness meaning mass-loading weight.

The fitting of the experimental impedance using the data for symmetric cells was carried out with Zview software (Scribner Associates, Inc., USA).[5] The equivalent circuit for fitting of impedance spectra at loading weights of 2, 4, 6 and 8 mg cm^{-2} was determined using a generalized finite length Warburg element open circuit terminus (Wo) for descriptive purposes. The fitting at high loading weight of 12 and 14 mg cm^{-2} was used as the equivalent circuit that connects parallel circuit of constant-phase element and resistance components in series with Wo in consideration of impedance spectra at high frequencies of over 1 kHz. R_{ion} was calculated using equation (S2) from the resistance values obtained by the fitting. All of the internal resistances obtained by fitting were normalized per unit geometric area of the electrode. Ionic conductivities in pores were calculated from R_{ion} considering electrode thickness.

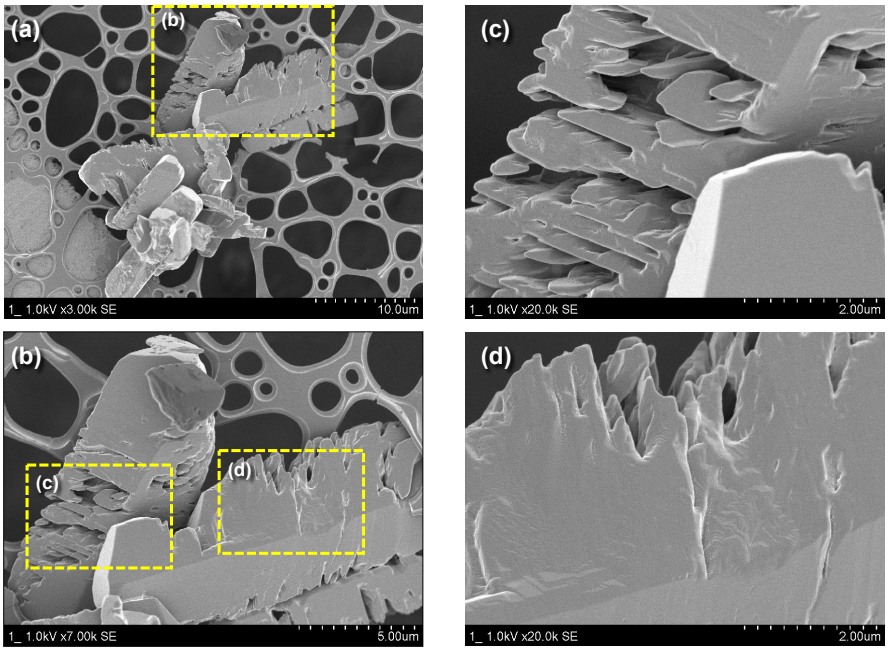

Fig. S1 SEM images of pristine 2,6-Naph(COOLi)$_2$ crystals.

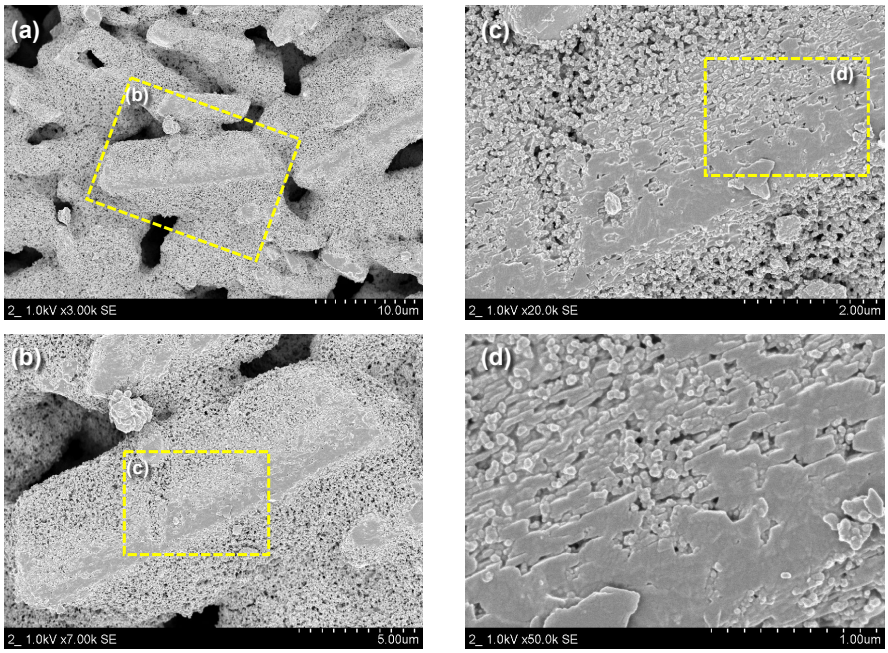

Fig. S2 Surface SEM images of porous 2,6-Naph(COOLi)$_2$ electrodes prepared using amphiphilic CMC binder.

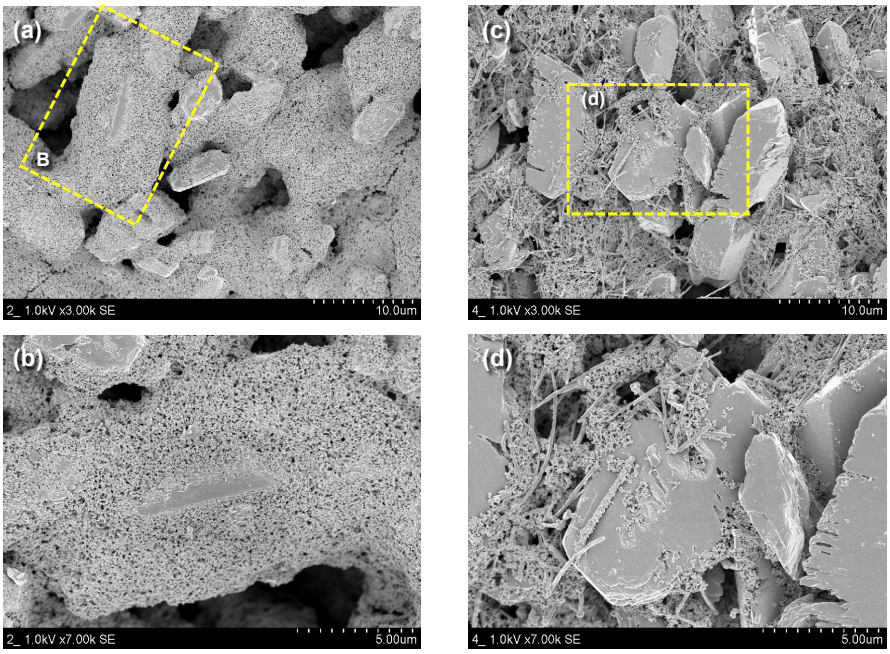

Fig. S3 Surface SEM images of porous 2,6-Naph(COOLi)$_2$ electrodes prepared using (a), (b) amphiphilic CMC binder and (c), (d) PVDF binder. The electrodes prepared using PVDF binder contained vapor-grown carbon fiber as the conductive carbon agent.

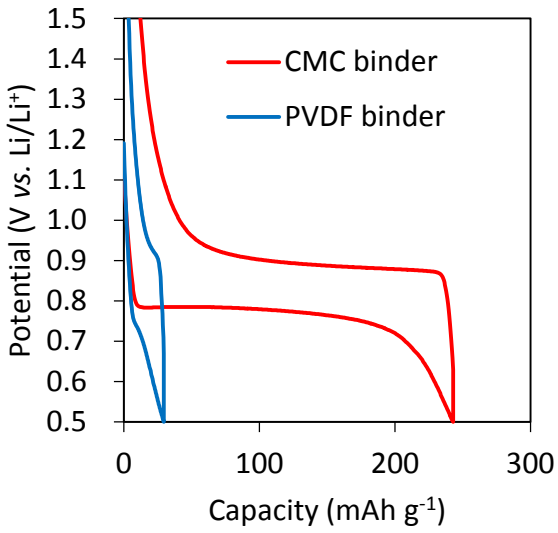

Fig. S4 Steady-state charge–discharge profiles of Li/2,6-Naph(COOLi)$_2$ cells prepared using CMC and PVDF at a rate corresponding to full charge of the theoretical capacity of the respective active materials in 10 h. The two electrodes had the same composition (active material : carbon black = 85 : 15 wt%) and loading weight of active material (*ca.* 2 mg cm^{-2}).

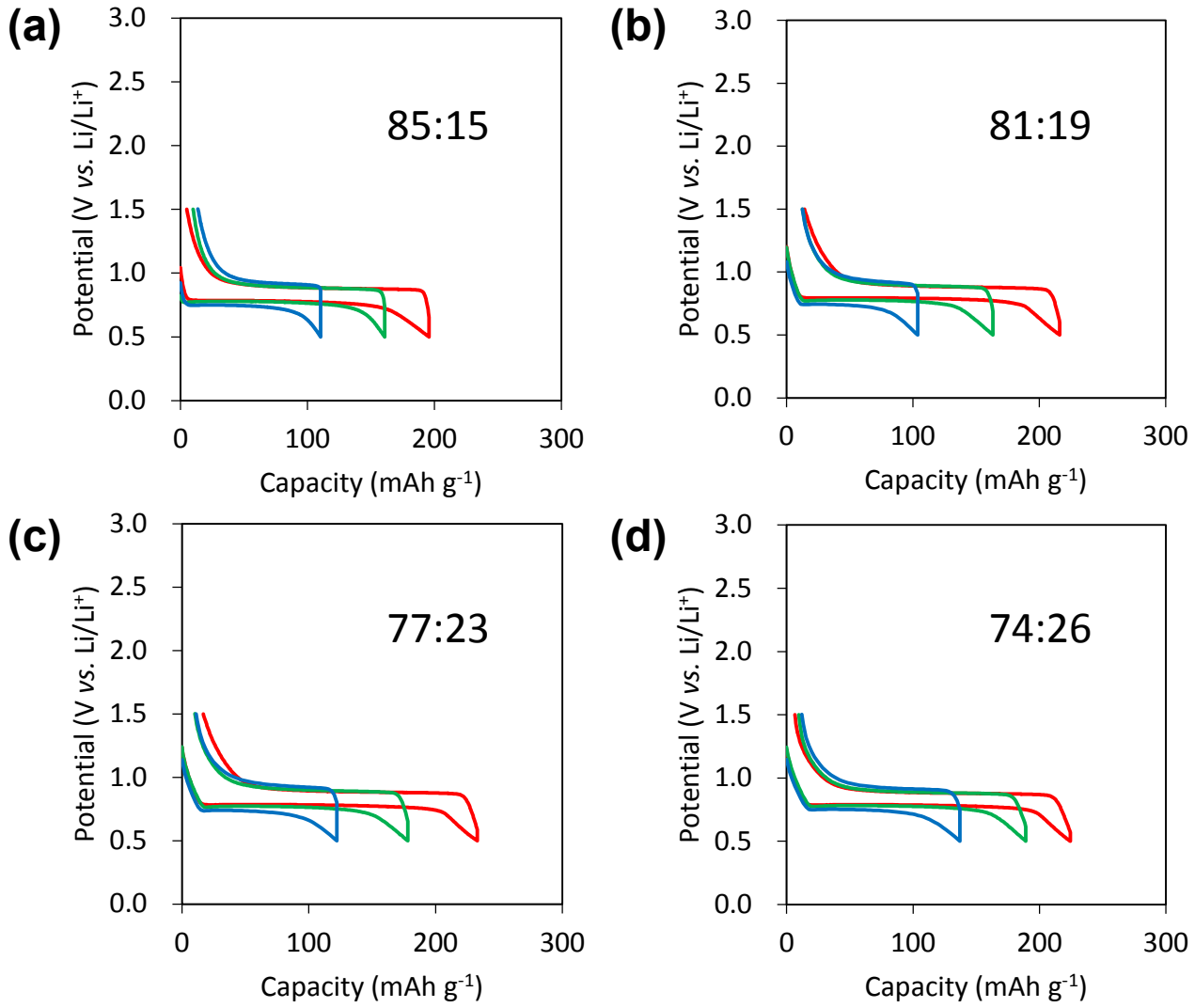

Fig. S5 Charge–discharge curves for Li/2,6-Naph(COOLi)$_2$ cells at different C rates. The ratio of active material to conductive nanocarbon was (a) 85:15, (b) 81:19, (c) 77:23 and (d) 74:26. The charge–discharge curves of red, green and blue are C/10 (10 h for discharge), C/5 (5 h for discharge) and C/2 (2 h for discharge), respectively.

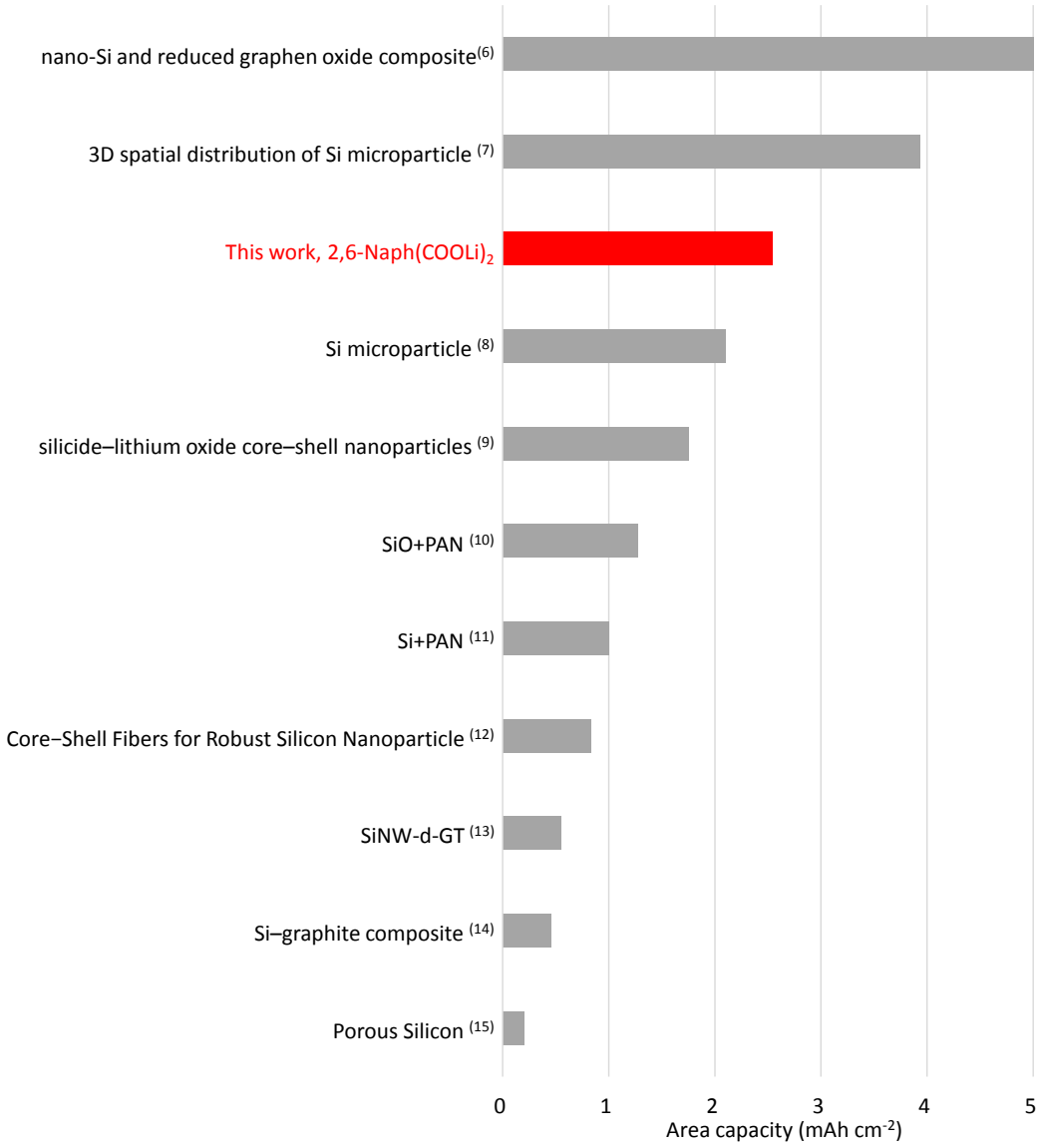

Fig. S6 Comparison of the area capacity of the 2,6-Naph(COOLi)$_2$ electrode with reported high-area-capacity Si-based electrode materials (ref.[6-15]) known to possess a high specific theoretical capacity (4200 mAh g^{-1}) for Li-ion batteries.

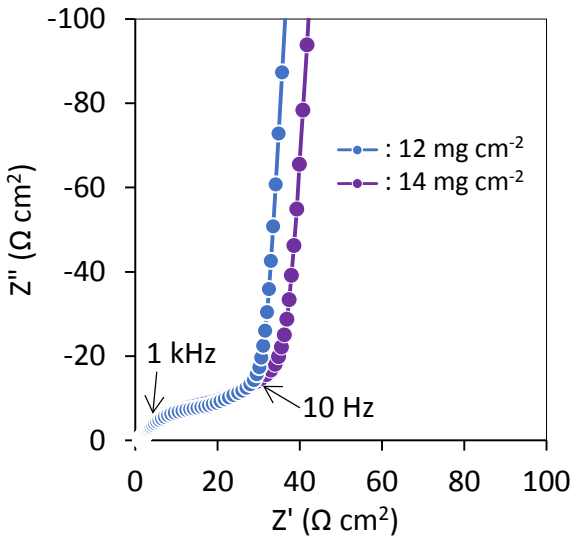

Fig. S7 Nyquist plot for a symmetric cell containing two porous 2,6-Naph(COOLi)$_2$ electrodes at loading weights of ca. 12 and 14 mg cm^{-2} in 1.0 M $LiPF_6$ in EC/DMC/EMC (volume ratio of 30/40/30) at 25 °C.

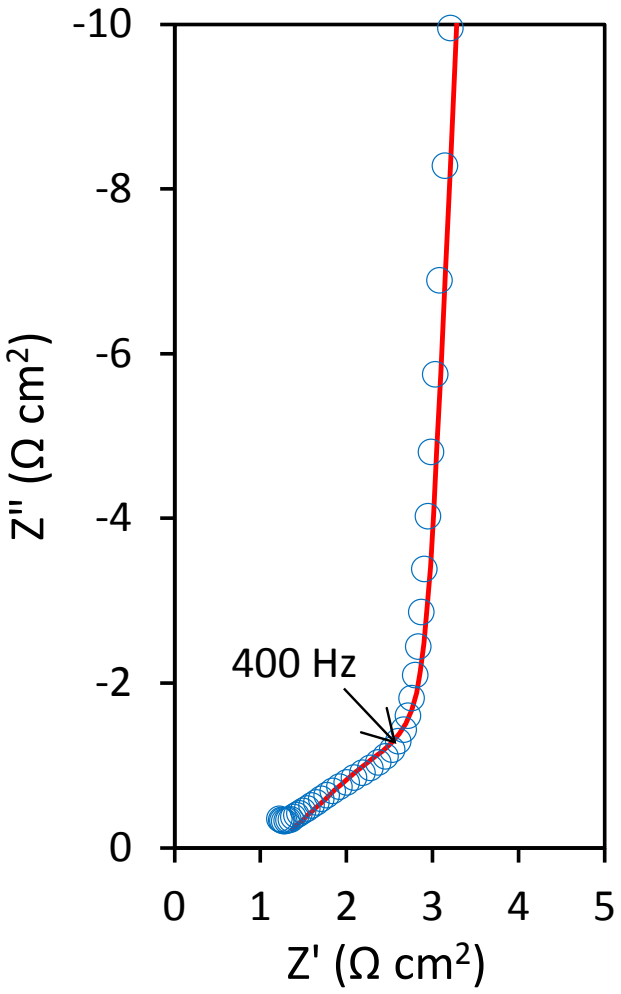

Fig. S8 Nyquist plot for a symmetric cell containing two porous 2,6-Naph(COOLi)$_2$ electrodes in 1.0 M $LiPF_6$ in EC/DMC/EMC (volume ratio of 30/40/30) at 25 °C (circles). Loading weight was *ca.* 2 mg cm^{-2}. The Nyquist plot consisted of the real part (Z'_ω) on the x-axis and - imaginary part (Z''_ω) on the y-axis. Solid lines are the best-fitting results with the equivalent circuits obtained using generalized finite length Warburg element open circuit terminus.[2]

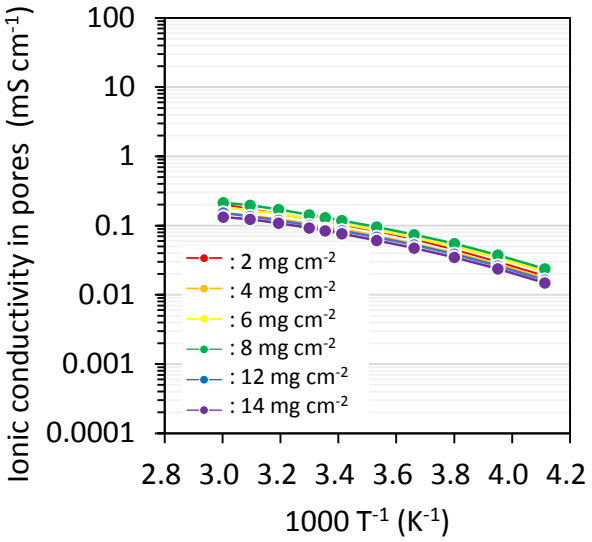

Fig. S9 Temperature dependence of the ionic conductivity in the pores of the porous 2,6-Naph(COOLi)$_2$ electrodes with different loading weights obtained by fitting.

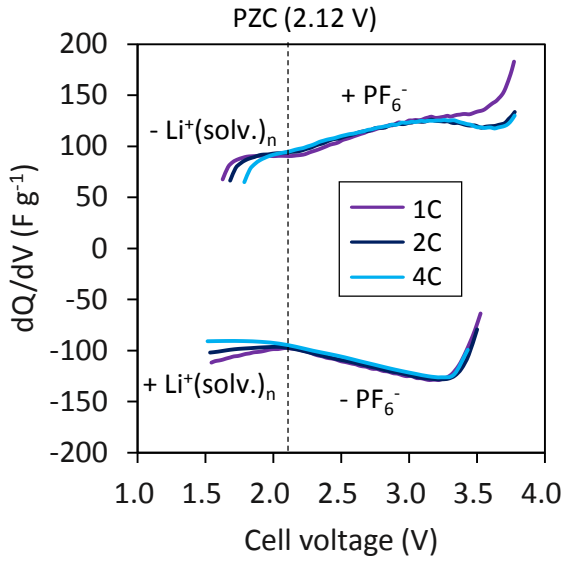

Fig. S10 Differential capacity dQ/dV plots of asymmetric capacitors containing Li-pre-doped 2,6-Naph(COOLi)$_2$ negative and AC positive electrodes at a rate corresponding to full charge in 1.0 (1C), 0.5 (2C) and 0.25 (4C) h. The capacity ratio of the negative electrode to the positive electrode was 2.7. The plots show a butterfly-like shape and potential of zero charge[16]. This means that the AC positive electrode is available for the electric double-layer capacitance of both PF_6^- anions and Li^+ cations.

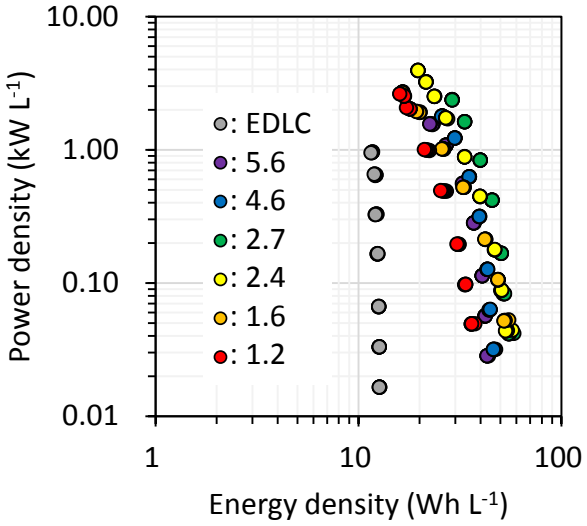

Fig. S11 Volumetric energy *versus* power of the proposed asymmetric capacitor at various capacity ratio balances of the 2,6-Naph(COOLi)$_2$ negative and AC positive electrodes, with that of an AC-based EDLC for comparison. The values in the figure are ratios of the negative electrode capacity to the positive electrode capacity obtained by changing the loading weight. The cell with a capacity ratio of the negative electrode to the positive electrode of 2.7 was chosen as the optimum composition in this study.

References

1. N. Ogihara, S. Kawauchi, C. Okuda, Y. Itou, Y. Takeuchi and Y. Ukyo, *J. Electrochem. Soc.*, 2012, **159**, A1034-A1039.
2. N. Ogihara, Y. Itou, T. Sasaki and Y. Takeuchi, *J. Phys. Chem. C*, 2015, **119**, 4612-4619.
3. R. de Levie, *Electrochim. Acta*, 1963, **8**, 751-780.
4. R. de Levie, *Electrochim. Acta*, 1964, **9**, 1231-1245.
5. D. Johson, *Scribner Associates, Inc., Southern Pines*, 2009.
6. B. P. N. Nguyen, N. A. Kumar, J. Gaubicher, F. Duclairoir, T. Brousse, O. Crosnier, L. Dubois, G. Bidan, D. Guyomard and B. Lestriez, *Adv. Energy Mater.*, 2013, **3**, 1351-1357.
7. Z. Chen, C. Wang, J. Lopez, Z. Lu, Y. Cui and Z. Bao, *Adv. Energy Mater.*, 2015, **5**, 1401826.
8. C. Wang, H. Wu, Z. Chen, M. T. McDowell, Y. Cui and Z. Bao, *Nat. Chem.*, 2013, **5**, 1042-1048.
9. J. Zhao, Z. Lu, N. Liu, H. W. Lee, M. T. McDowell and Y. Cui, *Nat. Commun.*, 2014, **5**, 5088.
10. S. Komaba, K. Shimomura, N. Yabuuchi, T. Ozeki, H. Yui and K. Konno, *J. Phys. Chem. C*, 2011, **115**, 13487-13495.
11. S. Komaba, N. Yabuuchi, T. Ozeki, Z.-J. Han, K. Shimomura, H. Yui, Y. Katayama and T. Miura, *J. Phys. Chem. C*, 2012, **116**, 1380-1389.
12. T. H. Hwang, Y. M. Lee, B. S. Kong, J. S. Seo and J. W. Choi, *Nano Lett.*, 2012, **12**, 802-807.
13. B. Wang, X. Li, X. Zhang, B. Luo, Y. Zhang and L. Zhi, *Adv. Mater.*, 2013, **25**, 3560-3565.
14. Z.-J. Han, N. Yabuuchi, K. Shimomura, M. Murase, H. Yui and S. Komaba, *Energy Environ. Sci.*, 2012, **5**, 9014.
15. S. R. Gowda, V. Pushparaj, S. Herle, G. Girishkumar, J. G. Gordon, H. Gullapalli, X. Zhan, P. M. Ajayan and A. L. Reddy, *Nano Lett.*, 2012, **12**, 6060-6065.
16. S. Shiraishi, H. Kurihara, L. Shi, T. Nakayama and A. Oya, *J. Electrochem. Soc.*, 2002, **149**, A855.